Journal of Mines, Metals and Fuels, *73(8): 2557-2567; 2025. DOI: 10.18311/jmmf/2025/49260*

Print ISSN : 0022-2755

Journal of Mines, Metals and Fuels

Contents available at: *www.informaticsjournals.co.in/index.php/jmmf*

Optimization of Dynamic Voltage Stability with a Novel Intelligent Controller for Multiple PV-DSTATCOM Systems

Vinayak Gaikwad* and Prerna Goswami

Institute of Chemical Technology, Mumbai - 400019, Maharashtra, India; gaikwadvinu1109@gmail.com

Abstract

This research presents an innovative PV-DSTATCOM smart control system designed to enhance dynamic voltage stability in multiple photovoltaic (PV) solar systems. The proposed system efficiently manages PV solar systems in various operational modes, including DSTATCOM functionality and PV power generation. During disturbances, smart control temporarily halts active power generation in selected solar systems, utilizing them as reactive power compensators to stabilize voltage levels. Once the disturbance is resolved, the system seamlessly restores the solar systems to their pre-disturbance PV power generation mode. To evaluate the effectiveness of the proposed controller, extensive simulations are conducted using EMTDC/PSCAD under various scenarios. The results confirm the system's ability to significantly enhance power system stability and improve dynamic performance. This approach demonstrates a practical and reliable solution for integrating PV systems into modern power networks while ensuring voltage stability and grid resilience.

Major Findings: *This research develops a smart PV-DSTATCOM system that switches PV units between power generation and reactive support to enhance voltage stability. Using full-PV, partial-, and full-STATCOM modes, it improves stability under load variations, offering a cost-effective solution without needing additional FACTS devices.*

Keywords: *Photovoltaic System, PSCAD Software, Smart Control, Static Compensator, Voltage Stability*

1.0 Introduction

Considering that non-renewable energy sources such as oil and gas will run out and the problems caused by the use of these energies, such as climate change, air pollution, and environmental destruction, the use of renewable energy sources is very important[1]. Renewable energy sources are clean and have the least damage to the environment. Meanwhile, these resources are endless and will be usable for many years and future generations. Currently, Photovoltaic solar systems have the fastest growth acceleration among renewable energy technologies. The entry of PV farms into the power system has many advantages. According to the results of researchers' studies related to PV integration into networks, the study and analysis of the relationship between the widespread presence of these resources and the problem of power system sustainability seem necessary[2,3]. With the increasing size and magnitude of the power system, parts of the system that are responsible for electricity generation, such as synchronous and wind generators, are susceptible to electromechanical fluctuations[4].

Boosting the gearbox voltage also amplifies the power system's dynamic variations. A power plant or synchronous generator might experience these variations.

**Author for correspondence*

When small fluctuations occur in the power system, power control systems like the Power System Stabilizer (PSS) and the governor can handle the problem. However, when large fluctuations occur, it is even more effective to have equipment that can improve dynamic stability in addition to these controllers[5]. Our goal in writing this study is to contribute to making the power system more dynamically stable in terms of voltage through the novel idea of PV-STATCOM and the suggested smart control, which will keep voltage levels within the permitted range even when there is a disturbance[6]. It was suggested in 2009[7] to use PV solar farms as STATCOM. The idea behind this technology is to use the inverter for reactive power adjustment and temporarily halt the active power generation of the solar power plant whenever there is a disturbance. Upon completion of the tasks required by the network, the solar farm will resume its usual operation. In reference[8], the use of PV-STATCOM to decrease TOV. This is demonstrated when there are asymmetrical defects. The article delves into the use of PV-STATCOM to mitigate Power Oscillation Damping (POD) in multiple power systems[9]. Another example[10] which shows how PV-STATCOM can help reduce Sub-Synchronous Resonance (SSR) in a steam turbine by compensating the transmission line with a series capacitor. The next section of this article details the suggested controller and PV-STACOM, and then uses EMTDC/PSCAD software simulations to test them.

2.0 PV-STATCOM Description

Figure 1 shows the typical 24-hour active and reactive power production of a PV-STATCOM solar system. What follows is a description of the operational modes:

i. In full-PV mode, the PV-STATCOM software only delivers actual power. The functioning of this is comparable to that of traditional PV systems.
ii. In partial-STATCOM mode, the PV system can create reactive power during the day in addition to active power.
iii. Full STATCOM mode: As the sun goes down, the PV inverters' full power can be directed towards reactive power compensation, ensuring a stable voltage. During the day, if there's an interference that the partial-STATCOM mode can't handle, the smart control will stop making real power and use all the capacity for reactive power adjustment. The PV system resumes its regular active power generation once the disturbance has been eliminated[11].

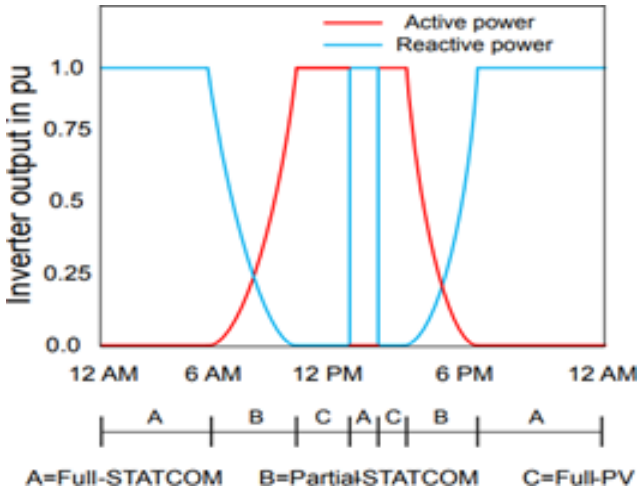


Figure 1. Output of a PV-STATCOM system during 24 hours[11].

3.0 The Study System

Exhibited in Figure 2 is the system research. The LB system is equipped with two PV solar systems, each with a 4-kW capacity.

They function in three modes—full-PV, partial-STATCOM, and full-STATCOM—by using the suggested smart control and in accordance with the needs of the power system. Any disturbances in the LB will be caused by a 25 KW fixed load or a variable load with varying stages.

3.1 Control Units of PV-STATCOM Systems

Figure 2 demonstrates the control units of each PV-STATCOM system, which includes PV panels, an inverter, a filter, and a control unit. The control system includes an AC voltage controller, a DC voltage controller, a current controller and other blocks which ultimately provide inverter pulses[12,13]. The task of controlling the operation modes of each PV-STATCOM is the responsibility of the smart controller. The control units are given.

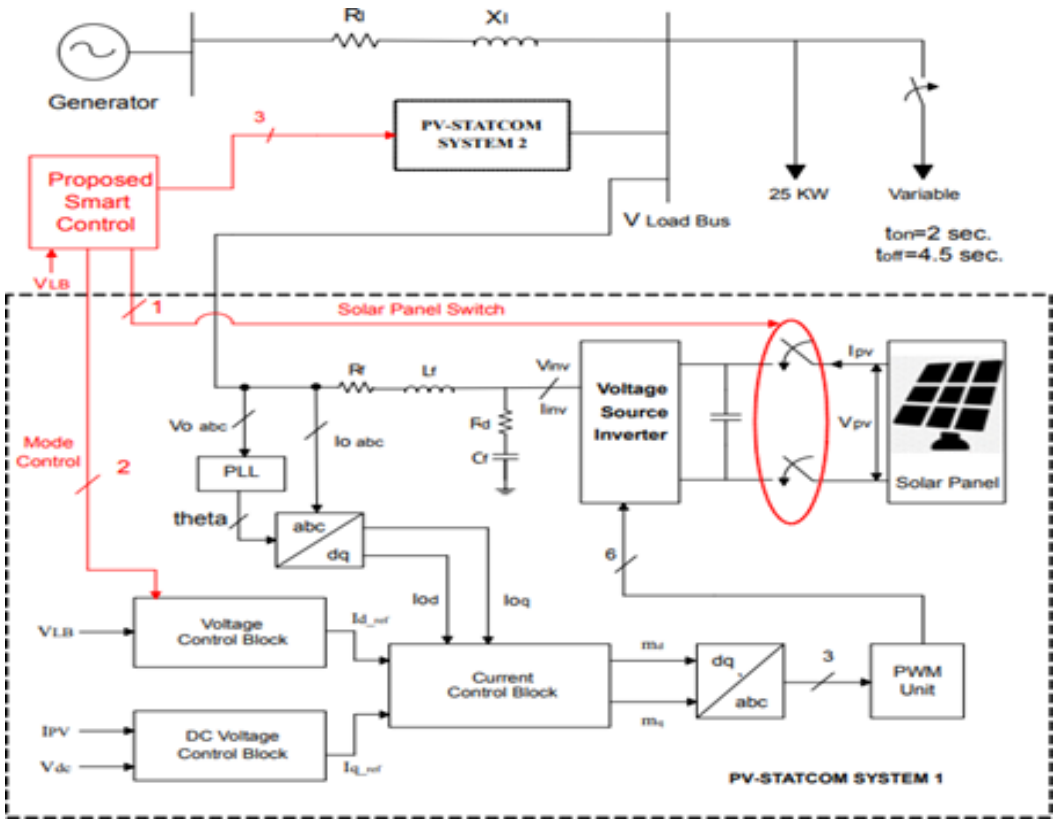


Figure 2. Modelling of the study system with the proposed mechanism.

3.2 Current Controller

The current controller components are demonstrated in Figure 3. By comparing i_d and i_q with their reference values, Error signals are obtained. These signals pass through a pi controller whose parameters are adjusted by a trial-and-error method[14,15]. Finally, the md and mq parameters are obtained, and after converting to m_{abc} to generate IGBT pulses, it is compared with the carrier signal[16]. The current control is responsible for adjusting the output voltage level of the inverter.

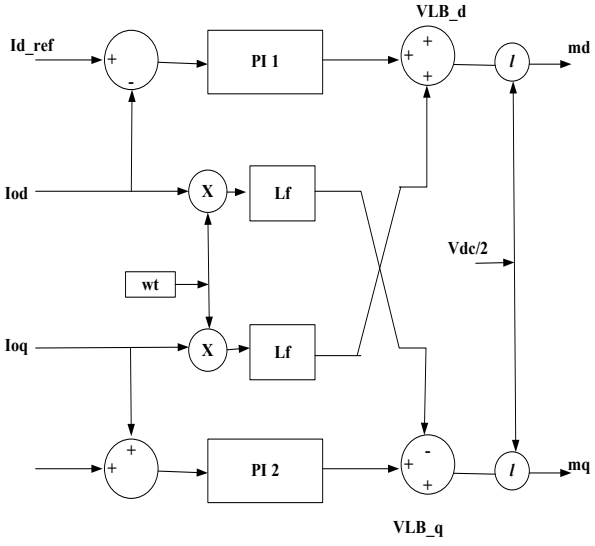


Figure 3. Current-control block.

The output active and reactive power of PV-STATCOM systems in the d_q frame are as follows:

$$P_0(t) = \frac{3}{2}\left(V_{lb-d}(t) I_{od}(t) + V_{lb-q}(t) I_{oq}(t)\right) \quad (1)$$

$$Q_0(t) = \frac{3}{2}\left(-V_{lb-d}(t) I_{oq}(t) + V_{lb-q}(t) I_{od}(t)\right) \quad (2)$$

I_o–d_q and V_{lb}–d_q are the output current of the PV-STATCOM system and the LB voltage in the dq frame, respectively. The output active power of the inverter is controlled by I_o–d, and the output reactive power is controlled by I_o–d. Due to the small amount of the shunt filter current, the output current of the PV-STATCOM

system is considered equal to the inverter current[17,18]. At the AC side of the inverter, we have

$$V_{inv} = R_f I_{inv} + L_f \frac{dI_{inv}}{dt} + V_{lb} \quad (3)$$

The voltage at the AC side of the inverter is controlled as follows:

$$L_{inv,abc} = \frac{V_{dc}}{2} m_{abc} \quad (4)$$

Where V_{dc} and mabc are the DC bus voltage and modulation index, respectively. Hence, the current of inverters in the dq frame

$$L_f \frac{dI_{inv-d}}{dt} = L_f \omega(t) I_{inv-q} - R_f I_{inv-d} + \frac{V_{dc}}{2} m_d - V_{lb-d} \quad (5)$$

$$L_f \frac{dI_{inv-q}}{dt} = -L_f \omega(t) I_{inv-d} - R_f I_{inv-q} + \frac{V_{dc}}{2} m_q - V_{lb-q} \quad (6)$$

Where V_{lb}–d_q is the LB voltage, I_{inv}–d_q is the inverter current, and m_{dq} is the modulation indices in the d_q frame[19]. To linearize relations (5) and (6)

$$L_f \frac{dI_{inv-d}}{dt} + R_f I_{inv-d} = u_d \quad (7)$$

$$L_f \frac{dI_{inv-q}}{dt} + R_f I_{inv-q} = u_q \quad (8)$$

The modulation indices are obtained as follows:

$$m_d = \frac{2}{V_{dc}} \left(u_d - L_f \omega_0 I_{inv-q} + V_{lb-d} \right) \quad (9)$$

$$m_q = \frac{2}{V_{dc}} \left(u_q - L_f \omega_0 I_{inv-d} + V_{lb-q} \right) \quad (10)$$

After converting to the abc frame, m_d and m_q are compared with the carrier signal to generate IGBT pulses[20-22].

3.3 DC Voltage Controller

The DC voltage controller is shown in Figure 4. The MPPT

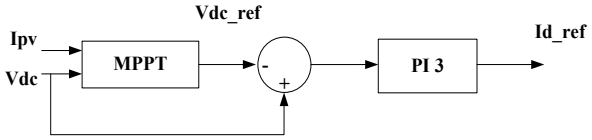


Figure 4. DC voltage control unit.

block generates V_{dc-ref} by using I_{pv} and V_{dc} as inputs to the controller. The I_{q-ref} current is generated when this value is compared with V_{dc}, and an error signal is generated after it passes through the PI controller[23,24].

3.4 Controller for Voltage

There are three ways that the voltage controller can operate:

- Full-PV: This mode is triggered by moving "S1" and "S2" to the "B" position. It represents the PV system operating normally when the LB voltage is within an acceptable range and the reactive power needs not be adjusted[25,26].
- Full-STATCOM: The voltage level at the LB is managed using this functional mode[27]. When the connection between the panels and the inverter is

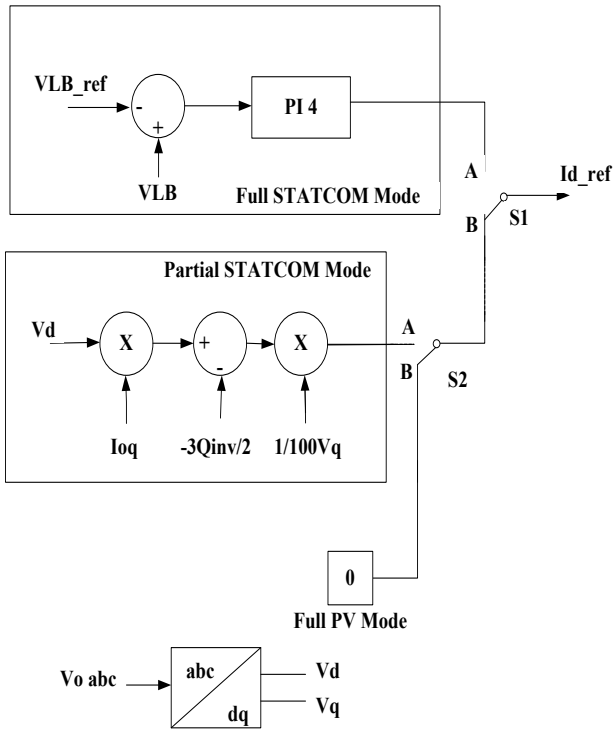


Figure 5. Voltage control unit.

broken, it is utilised to transfer reactive electricity back and forth between the grid and the inverter. To enter this mode, move the "S1" lever to the "A" position.

- Partial-STATCOM: This operating mode uses the inverter's remaining capacity to compensate for reactive power at the LB while controlling the voltage when the panels are connected to the inverter. To initiate this mode, move "S1" to position "B" and "S2" to position "A"[28]. In Figure 5, a voltage control device is shown.

4.0 The Proposed Smart Control

The proposed smart control performance is illustrated in Figure 6, which is a flow diagram. It all starts with taking readings of the LB's voltage. The smart control is in charge of deciding which of three modes (full-PV, partial-STATCOM, or full-STATCOM) to operate each solar system in accordance with the voltage value that has been measured. The smart control switches both systems to full-PV mode when there is no disturbance (big load, malfunction, etc.) and reactive power compensation is not necessary.

At each stage, the inverter's remaining capacity (Q_{rem}) is determined by the solar radiation. If there is a voltage drop or disturbance that causes the required reactive power to be less than Q_{rem}, the smart control will put one or two systems into partial-STATCOM mode. This will allow them to compensate for reactive power without interrupting the active power generation. Disconnecting the solar panels from the inverters using the smart control puts the entire capacity of the inverters to use controlling the voltage ($Q_{inv} = S_{inv}$) in the event that the required reactive power exceeds the remaining capacity of the systems and both systems must be in full-STATCOM mode due to an interference.

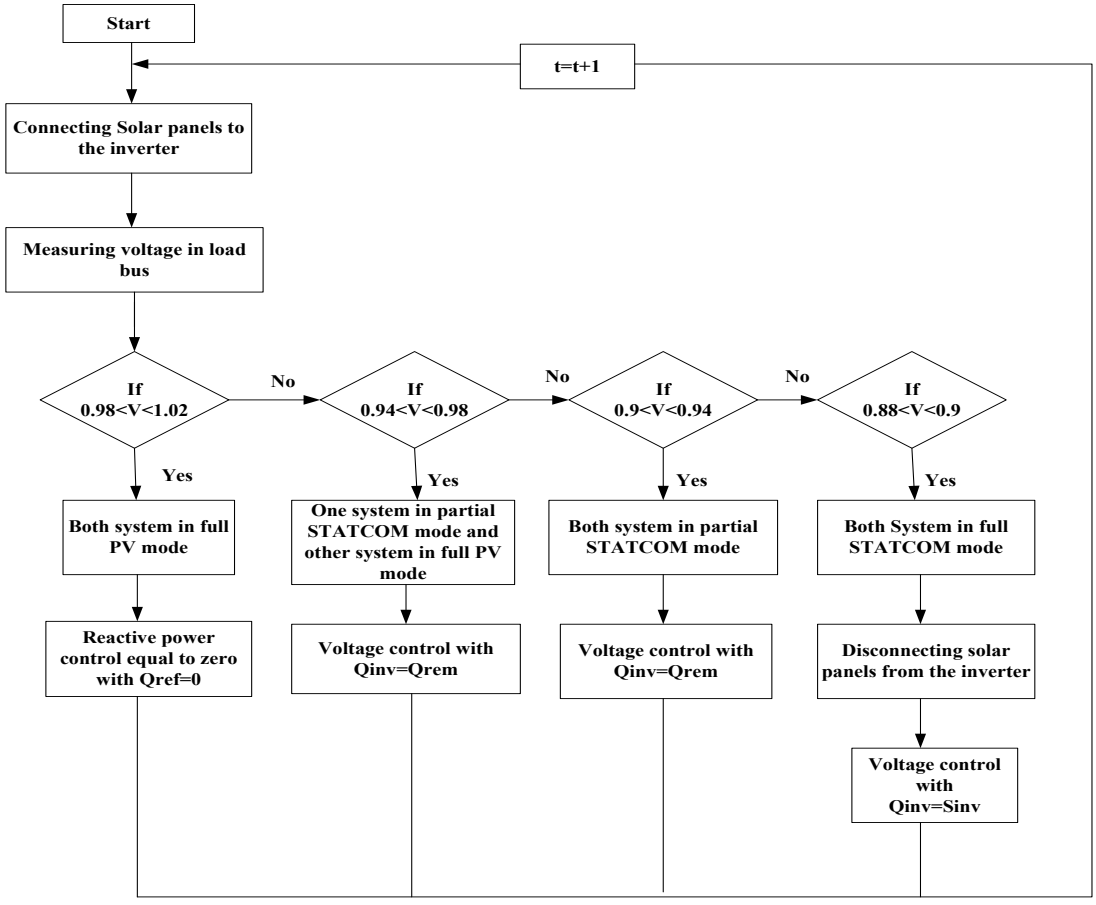


Figure 6. Flowchart of operation modes selector of proposed smart control.

5.0 Results and Discussion

In this section, the performance of the proposed smart control and PVSTATCOMs to improve dynamic voltage stability is presented. PSCAD/EMTDC software has been used to simulate the study system. The results are described as follows:

5.1 The Performance of the Smart Controller in Different Loads

The performance of smart control in the studied system is investigated under different loads. A 25kW load is connected to the LB, the voltage is in the appropriate

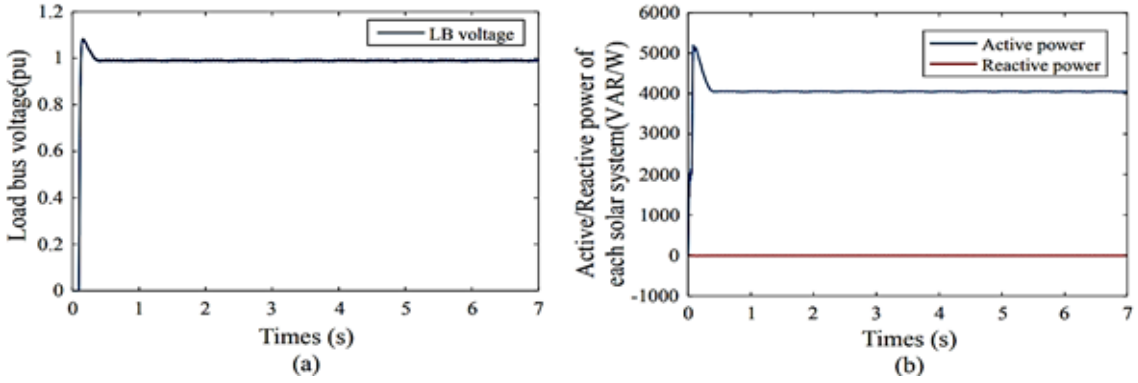


Figure 7. LB voltage and active/reactive power of each solar system (a) LB voltage (b) active and reactive power.

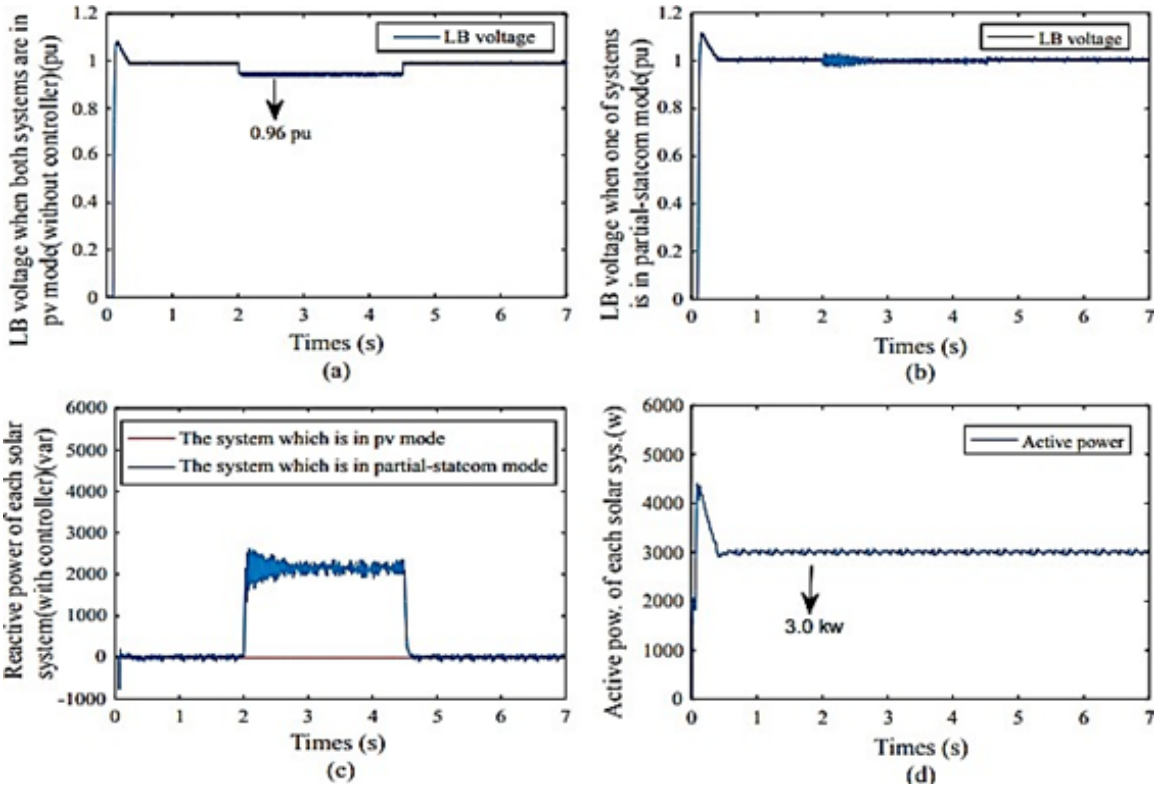


Figure 8. Responses of the system **(a)** LB voltage without controller, **(b)** LB voltage with controller, **(c)** reactive power of each system with the controller, and **(d)** active power of each system with the controller.

range, and there is no need for compensation; the results are illustrated in Figure 7:

Now, in addition to the 25-kW load, 6 kvar, 8 kvar and 16 kvar loads are connected to the LB in the time interval of 2.0 - 4.5 seconds, respectively. At the first step, by connecting of 6 kvar load, according to the need, the smart control puts one of the systems in partial-STATCOM mode and the other system in full PV mode. The responses of this step are shown in Figure 8.

In the second step, by connecting of 8 kvar load, the smart control puts both systems in Partial-STATCOM mode. The results of this step are demonstrated in Figure 9.

At the third step, upon connecting a 16 kvar load, the smart control dynamically adjusts both systems to full-STATCOM mode as needed. The responses to this step are depicted in Figure 10.

For \(t < 2.0 \) sec: The system operates normally under all conditions, maintaining a voltage of 1 per unit (pu) in the Load Bus (LB), with zero reactive power production during this interval.

For \(2.0 < t < 4.5 \) sec: Upon connecting 6 kvar, 8 kvar, and 16 kvar loads to the LB within this time interval, corresponding voltage drops occur in the LB, resulting in voltages of 0.96 pu, 0.93 pu, and 0.88 pu, respectively. The controller promptly detects these voltage drops in each mode, compensating accordingly by adjusting the reactive power output and transitioning each system (as described earlier) to partial-STATCOM and full-STATCOM modes. Through reactive power injection into the LB, the voltage is restored to an acceptable range.

For \(t > 4.5 \) sec: Following the disconnection of the large load, no further compensation is required. The system voltage returns to its pre-disturbance conditions. It is observed that increasing the load induces a voltage

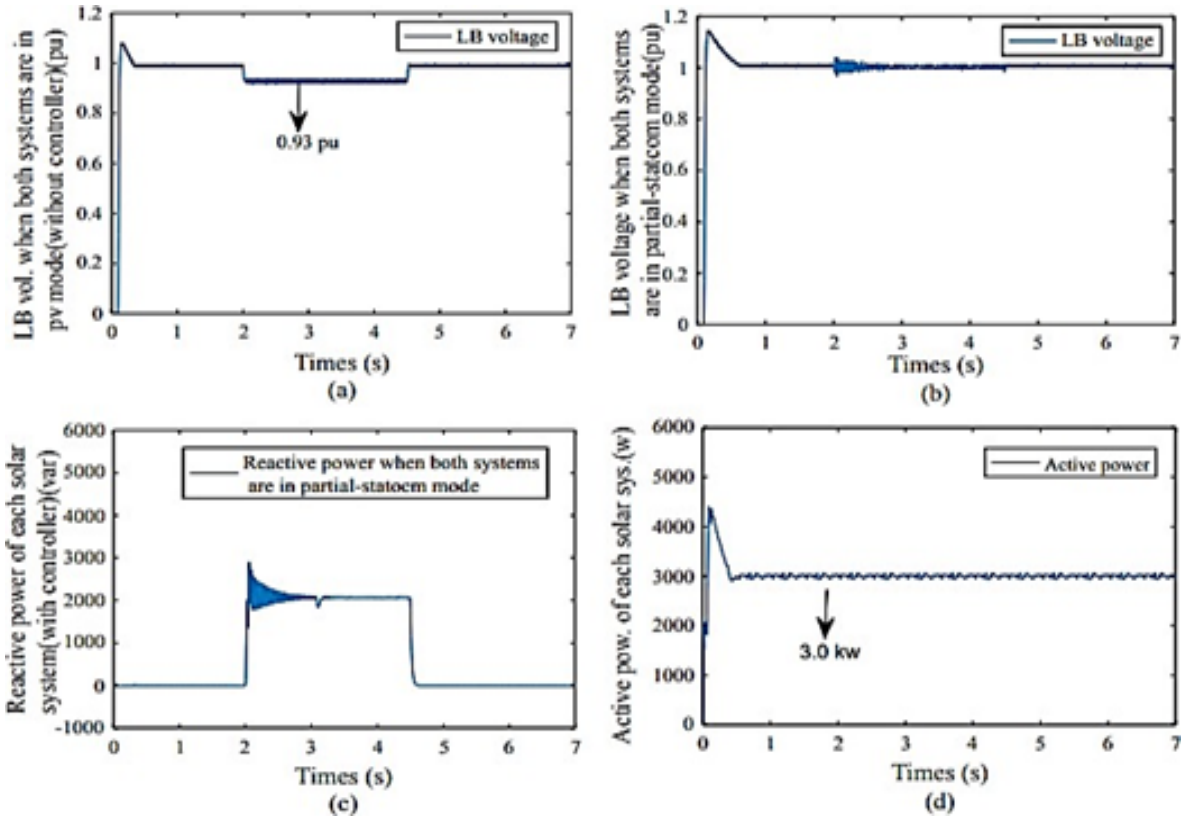


Figure 9. Responses of the system **(a)** LB voltage without controller, **(b)** LB voltage with controller, **(c)** reactive power of each solar system, and **(d)** active power of each solar system.

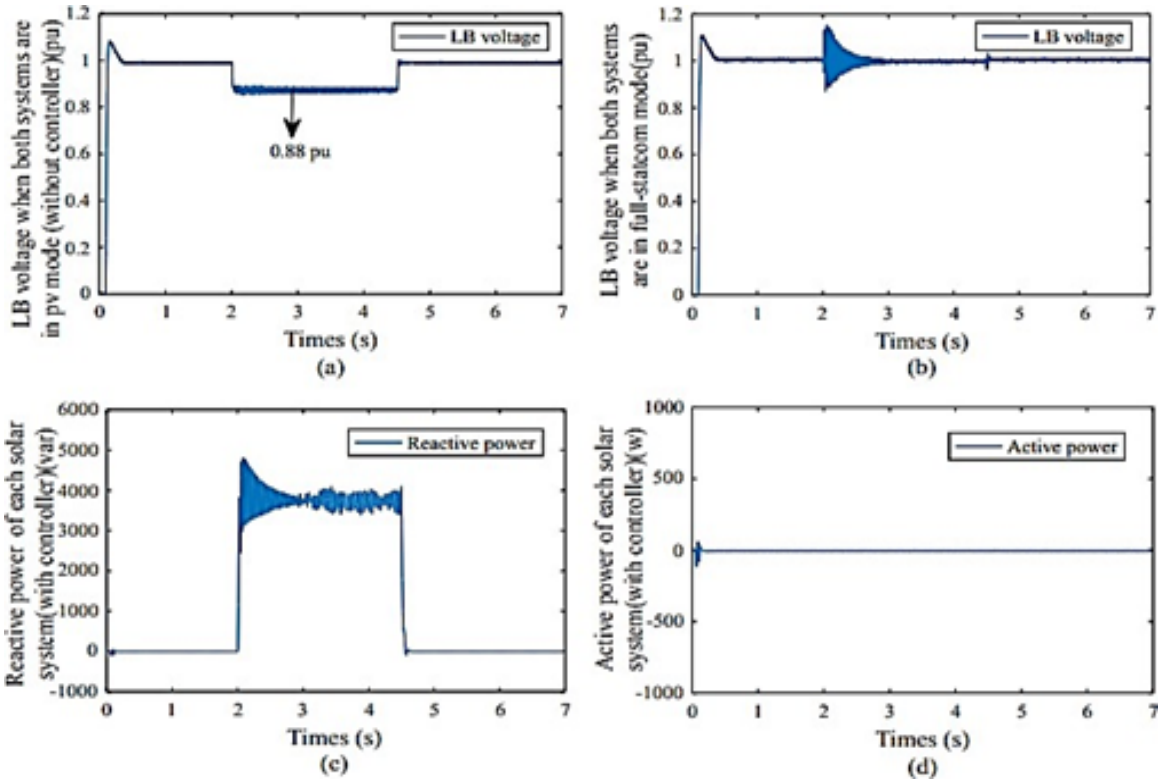


Figure 10. Responses of the system **(a)** LB voltage without controller, **(b)** LB voltage with controller, **(c)** reactive power of each system, and **(d)** active power of each solar system.

Table 1. The overshoot and settling results

States	System type	Overshoot (%)	Settling time (s)
1	System 1 and 2 full-PV	0	0
2	Sys.1 full-PV and sys. 2 partial-STATCOM	3	0.5
3	System1 and 2 partial-STATCOM	4	0.6
4	System1 and 2 full-STATCOM	12	1.3

drop, which the smart control swiftly detects and compensates for by injecting the necessary reactive power, resulting in the voltage stabilizing at an acceptable level with an overshoot and settling time. Moreover, higher voltage drops and injected reactive power led to increased overshoot and settling time. The overshoot and settling time results for all modes are summarized in Table 1.

5.2 Discussion

In this section, the reactive power compensation of the LB when one of the systems is in full-STATCOM mode is investigated, and the results are compared to the performance of smart control in compensation of the same load. For the first case, by connecting the variable load of 8 kvar, the system voltage in the time interval of 2.0-4.5 seconds drops from 1 pu to 0.93 pu. In this case, we put one of the PV systems in full-STATCOM mode and the other system in full PV mode. In this condition, by detecting the system voltage drop at t=2.0 Sec., by injecting 4 kvar reactive power into the system, which is in full-STATCOM mode, the system voltage is restored and brought to 1 pu. The results are demonstrated in Figure 11.

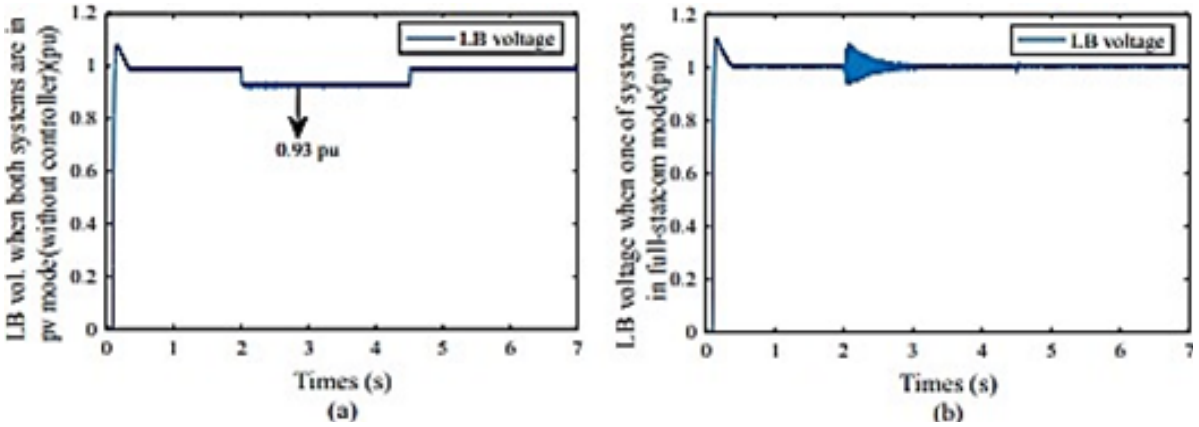


Figure 11. One system in full-STATCOM mode and the other system in full-PV mode **(a)** LB voltage without controller, and **(b)** LB voltage with controller.

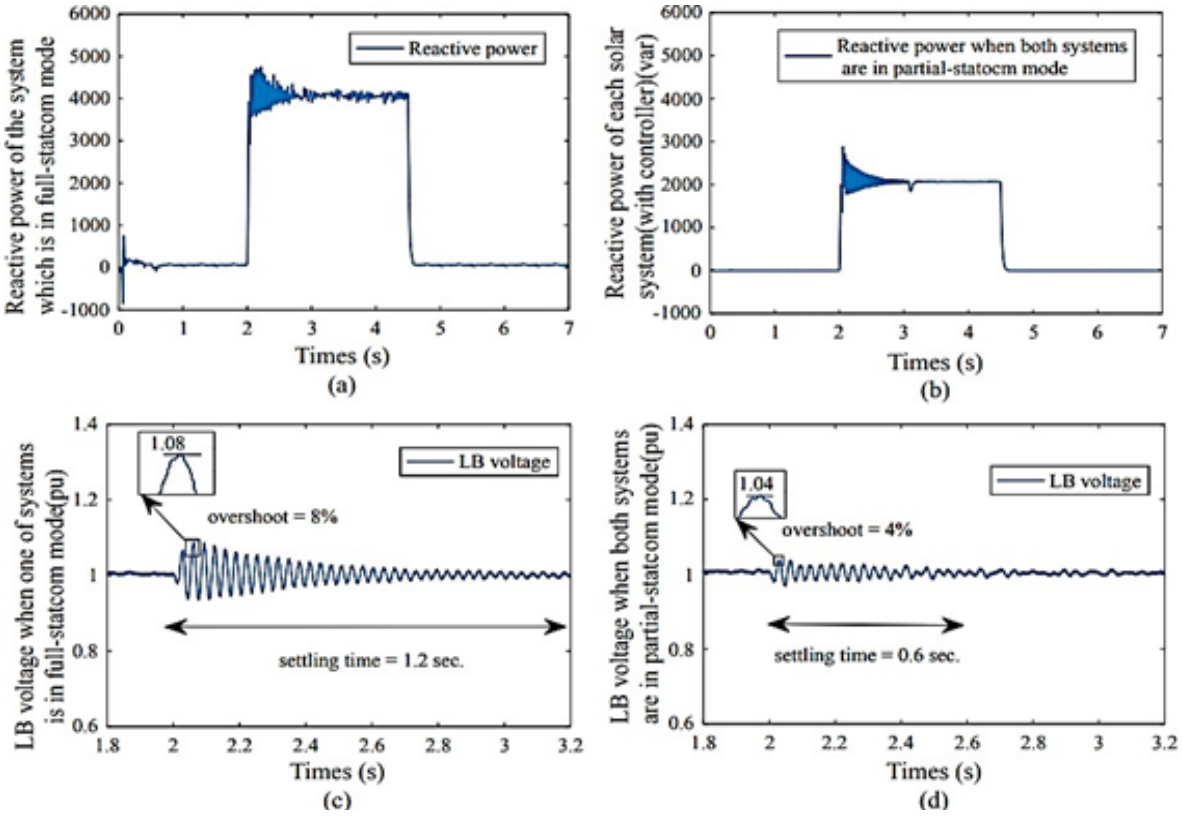


Figure 12. Comparison of the use of one solar system in full- STATCOM mode or both systems in partial- STATCOM mode for compensating the identical load **(a)** Reactive power injected by the system which is in full- STATCOM mode, **(b)** Reactive power of both systems which are in partial- STATCOM mode, **(c)** LB voltage with compensation by one system in full- STATCOM mode, **(d)** LB voltage with compensation by two systems in partial- STATCOM mode.

The comparative results to investigate the overshoot and settling time of the voltage at the LB when one of the systems is in full-STATCOM mode or both systems are in partial-STATCOM (smart control performance), in the compensation of the identical load, are demonstrated in Figure 12.

According to the results, the amount of compensation is the same in both modes and is equal to 4 kvar. In the first case, this value is provided by one PV system in full-STATCOM mode. In the second case, according to the performance of smart control, this value is provided when both systems are in partial-STATCOM mode (each system injects 2 kvar to the LB). It follows that when compensation is done when both systems are in partial STATCOM, the amount of overshoot and settling time are reduced by 50%. The results are demonstrated in Table 2.

Table 2. Overshoot and settling time of the LB voltage when one of the systems is in full- STATCOM mode or both systems are in partial- STATCOM modes

System type	Overshoot (%)	Settling time (s)
Sys.1 full--STATCOM and system 2 full-PV	8	1.2
System1 and 2 partial-STATCOM	4	0.6

6.0 Conclusion

This study introduces a novel smart control strategy for multiple Photovoltaic (PV)-Static Synchronous Compensator (STATCOM) systems aimed at enhancing the dynamic voltage stability of power systems. By integrating two solar systems with PV-STATCOM capabilities into the distribution network, the proposed controller orchestrates the operation of these systems across Three distinct modes: full-PV, partial-STATCOM, and full-STATCOM. Simulation results demonstrate the efficacy of the proposed controller in enhancing dynamic voltage stability amidst varying load conditions. Notably, this approach leverages existing infrastructure, circumventing the need for additional FACTS devices, thereby offering a cost-effective solution for improving power quality in inverter-based renewable energy systems.

In summary, the deployment of this innovative smart control strategy holds promise for enhancing the stability and reliability of power systems, particularly in the context of integrating renewable energy sources into existing grids.

7.0 References

1. Ocak M, Ocak Z, Bilgen S, Keleş S, Kaygusuz K. Energy utilisation, environmental pollution and renewable energy sources in Turkey. *Energy Convers Manag*. 2004; 45:845-64. https://doi.org/10.1016/S0196-8904(03)00192-4
2. Rafi MAH, Vo T, Nguyen PH. Effective integration of large-scale wind power using PV-STATCOM. *J Eng*. 2019; 2019:5303-7. https://doi.org/10.1049/joe.2018.9232
3. Magazzino C, Toma P, Fusco G, Valente D, Petrosillo I. Renewable energy consumption, environmental degradation and economic growth: the greener the richer? *Ecol Indic*. 2022; 139:108912. https://doi.org/10.1016/j.ecolind.2022.108912
4. Varma RK, Akbari M. Simultaneous fast frequency control and power oscillation damping by utilising PV solar system as PVSTATCOM. *IEEE Trans Sustain Energy*. 2020; 11:415-25. https://doi.org/10.1109/TSTE.2019.2892943
5. Varma RK, Mohan S. Mitigation of Fault-Induced Delayed Voltage Recovery (FIDVR) by PV-STATCOM. *IEEE Trans Power Syst*. 2020; 35(6):4251-62. https://doi.org/10.1109/TPWRS.2020.2991447
6. Karbouj H, Rather ZH, Pal BC. Adaptive voltage control for a large-scale solar PV power plant considering real-life factors. *IEEE Trans Sustain Energy*. 2020; 12(2):990-8. https://doi.org/10.1109/TSTE.2020.3029102
7. Varma RK, Siavashi EM. PV-STATCOM: a new smart inverter for voltage control in distribution systems. *IEEE Trans Sustain Energy*. 2018; 9:1681-91. https://doi.org/10.1109/TSTE.2018.2808601
8. Dhanapal S, Anita R. Voltage and frequency control of a standalone self-excited induction generator using photovoltaic system-based STATCOM. *J Circuits Syst Comput*. 2016; 25(4):1650031. https://doi.org/10.1142/S0218126616500316
9. Afsher PA, Kumar MVM, Mukundan CMN, Shyju K. A PV-DSTATCOM with adaptive DC-link voltage for grid integration and PQ enhancement. *IEEE Trans Ind Appl*. 2022; 58(5):6471-84. https://doi.org/10.1109/TIA.2022.3182641
10. Park J, *et al*. Frequency/voltage regulation with STATCOM with battery in a high-voltage transmission system. *IFAC-Pap Online*. 2016; 49(27):296-300. https://doi.org/10.1016/j.ifacol.2016.10.707
11. Suliman MY. Voltage profile enhancement in a distribution network using a static synchronous compensator STATCOM. *Int J Electr Comput Eng*. 2020;

10(4):3367-74. https://doi.org/10.11591/ijece.v10i4.pp3367-3374
12. Ali AJ, Suliman MY, Khalaf LA, Sultan NS. Performance investigation of a stand-alone induction generator based on STATCOM for wind power application. *Int J Electr Comput Eng*. 2020; 10(6):5570-8. https://doi.org/10.11591/ijece.v10i6.pp5570-5578
13. Rohouma W, Balog RS, Begovic MM, Peerzada AA. Capacitorless D-STATCOM for voltage profile improvement in a smart grid distribution network with high PV penetration. *Proc Int Conf Smart Grid (icSmartGrid)*. 2022; 3:155-9. https://doi.org/10.1109/icSmartGrid55722.2022.9848771
14. Canizares CA, *et al*. STATCOM modelling for voltage and angle stability studies. *Int J Electr Power Energy Syst*. 2003; 25(6):431-41. https://doi.org/10.1016/S0142-0615(02)00125-4
15. Moeini A, Kamwa I. Analytical concepts for reactive power-based primary frequency control in power systems. *IEEE Trans Power Syst*. 2016; 31:4217-30. https://doi.org/10.1109/TPWRS.2015.2511153
16. Chakraborty S, Mukhopadhyay S, Biswas SK. Optimal placement of PV-DSTATCOM-based EV charging stations with dynamic pricing. *IEEE Trans Ind Appl*. 2023; 59(6):7092-102. https://doi.org/10.1109/TIA.2023.3307345
17. Varma RK, Mohan S, McMichael-Dennis J. Multimode control of PV-STATCOM for stabilisation of remote critical induction motor. *IEEE J Photovoltaics*. 2020; 10:1872-81. https://doi.org/10.1109/JPHOTOV.2020.3013975
18. Varma RK, Khadkikar V, Seethapathy R. Nighttime application of PV solar farm as STATCOM to regulate grid voltage. *IEEE Trans Energy Convers*. 2009; 24:983-5. https://doi.org/10.1109/TEC.2009.2031814
19. Varma RK, Siavashi EM. Enhancement of solar farm connectivity with smart PV inverter PV-STATCOM. *IEEE Trans Sustain Energy*. 2019; 10:1161-71. https://doi.org/10.1109/TSTE.2018.2862405
20. Oda ES, Hamed AMAE, Ali A, Elbaset AA, Sattar MAE, Ebeed M. Stochastic optimal planning of distribution system considering integrated photovoltaic-based DG and DSTATCOM under uncertainties of loads and solar irradiance. *IEEE Access*. 2021; 9:26541-55. https://doi.org/10.1109/ACCESS.2021.3058589
21. Varma RK, Maleki H. PV solar system control as STATCOM (PVSTATCOM) for power oscillation damping. *IEEE Trans Sustain Energy*. 2019; 10:1793-803. https://doi.org/10.1109/TSTE.2018.2871074
22. Varma RK, Salehi R. SSR mitigation with a new control of PV solar farm as STATCOM (PV-STATCOM). *IEEE Trans Sustain Energy*. 2017; 8:1473-83. https://doi.org/10.1109/TSTE.2017.2691279
23. Varma RK, Siavashi EM, Mohan S, Vanderheide T. First in Canada, night and day field demonstration of a new photovoltaic solar-based Flexible AC Transmission System (FACTS) device PV-STATCOM for stabilising critical induction motor. *IEEE Access*. 2019; 7:149479-92. https://doi.org/10.1109/ACCESS.2019.2935161
24. Mishra E, Patil GH, Chavan SD, Jarad RS, Satarkar M, Thakare M, Maniyar K. Analysis of the impact of STATCOM on distance relay using MATLAB. *J Mines Met Fuels*. 2025; 73(3):743-50. https://doi.org/10.18311/jmmf/2025/48052
25. Mosaad MI, Ramadan HSM, Aljohani M, El-Naggar MF, Ghoneim SSM. Near-optimal PI controllers of STATCOM for an efficient hybrid renewable power system. *IEEE Access*. 2021; 9:34119-30. https://doi.org/10.1109/ACCESS.2021.3058081
26. Singh B, Kandpal M, Hussain I. Control of grid-tied smart PV-DSTATCOM system using an adaptive technique. *IEEE Trans Smart Grid*. 2018; 9(5):3986-93. https://doi.org/10.1109/TSG.2016.2645600
27. P A, SK, MK, MV. An enhanced operation of PV-DSTATCOM. *Proc IEEE Int Conf Power Electron Drives Energy Syst (PEDES)*. Jaipur, India; 2020:1-6. https://doi.org/10.1109/PEDES49360.2020.9379748
28. Kumar R, *et al*. Performance assessment of the two metaheuristic techniques and their hybrid for power system stability enhancement with PV-STATCOM. *Neural Comput Appl*. 2022; 34(5):3723-44. https://doi.org/10.1007/s00521-021-06637-9